Biochimica et Biophysica Acta 1777 (2008) 676–683

Contents lists available at ScienceDirect

Biochimica et Biophysica Acta

journal homepage: www.elsevier.com/locate/bbabio

Quantification of the electrochemical proton gradient and activation of ATP synthase in leaves

Pierre Joliot *, Anne Joliot

Institut de Biologie Physico-Chimique, CNRS, UMR 7141, Université Pierre et Marie-Curie, 13, rue Pierre-et-Marie Curie, 75005 Paris, France

ARTICLE INFO

Article history:
Received 4 February 2008
Received in revised form 31 March 2008
Accepted 4 April 2008
Available online 12 April 2008

Keywords:
ATP synthase
Electrochemical proton gradient
Membrane potential

ABSTRACT

We have developed a new method to quantify the transmembrane electrochemical proton gradient present in chloroplasts of dark-adapted leaves. When a leaf is illuminated by a short pulse of intense light, we observed that the light-induced membrane potential changes, measured by the difference of absorption (520 nm–546 nm), reach a maximum value (~190 mV) determined by ion leaks that occur above a threshold level of the electrochemical proton gradient. After the light-pulse, the decay of the membrane potential follows a multiphasic kinetics. A marked slowdown of the rate of membrane potential decay occurs ~100 ms after the light-pulse, which has been previously interpreted as reflecting the switch from an activated to an inactivated state of the ATP synthase (Junge, W., Rumberg, B. and Schröder, H., Eur. J. Biochem. 14 (1970) 575–581). This transition occurs at ~110 mV, thereby providing a second reference level. On this basis, we have estimated the $\Delta\tilde{\mu}_{H^+}$ level that pre-exists in the dark. Depending upon the physiological state of the leaf, this level varies from 40 to 70 mV. In the dark, the $\Delta\tilde{\mu}_{H^+}$ collapses upon addition of inhibitors of the respiratory chain, thus showing that it results from the hydrolysis of ATP of mitochondrial origin. Illumination of the leaf for a period longer than several seconds induces a long-lived $\Delta\tilde{\mu}_{H^+}$ increase (up to ~150 mV) that reflects the light-induced increase in ATP concentration. Following the illumination, $\Delta\tilde{\mu}_{H^+}$ relaxes to its dark-adapted value according a multiphasic kinetics that is completed in more than 1 h. In mature leaf, the deactivation of the Benson–Calvin cycle follows similar kinetics as $\Delta\tilde{\mu}_{H^+}$ decay, showing that its state of activation is mainly controlled by ATP concentration.

1. Introduction

According to the chemiosmotic theory, ATP synthesis is driven by a transmembrane electrochemical proton gradient denoted as $\Delta\tilde{\mu}_{H^+}$ [1,2]. In chloroplasts, ATP synthesis is promoted by a membrane-bound F_0F_1 ATP synthase that couples the transfer of H^+ across the membrane to the synthesis of ATP. Conversely, it has been shown that, in unicellular algae [3–5] the hydrolysis of ATP results in the presence of a permanent electrochemical proton gradient $\Delta\tilde{\mu}_{H^+}$ in the dark. Under aerobic conditions, this transmembrane potential has been ascribed to the hydrolysis of ATP of mitochondrial origin [6] evidencing the exchange of nucleotides between different cellular compartments, mitochondria, cytoplasm and chloroplasts. In this paper, we present new approaches based on the measurement of the membrane potential changes induced by a pulse of strong light to characterize the permanent $\Delta\tilde{\mu}_{H^+}$ level in dark-adapted or pre-illuminated leaves.

Another issue addressed in this paper deals with the activation process of the ATP synthase in vivo. It is known that an electrochemical proton gradient is required to activate the ATP synthase in addition to supply energy for ATP synthesis [7,8]. The magnitude of this $\Delta\tilde{\mu}_{H^+}$ is strongly decreased by the reduction of a disulfide bridge located in the γ subunit of the F_1 complex [9–12]. In addition, Junge et al. evidenced, in isolated thylakoids, the necessity for a critical membrane potential to activate the ATP synthase [13,14]. These authors observed that after illumination by a series of flashes, the decay of the light-induced membrane potential is biphasic. They proposed that the break between the first phase (completed in ~100 ms) and the second one reflects a transition between a high and a low level for ATP synthase activity. Such a threshold potential for the activation of the ATP synthase has also been characterized in dark-adapted unicellular algae [15,16] and leaves [15,16]. Junesh and Gräber [12] and Strelow and Rumberg [17], have quantitatively analyzed the activation of ATP synthase in its oxidized or reduced form as a function of ΔpH. The half-maximum activation levels of the oxidized and reduced states of the ATP synthase are ΔpH=2.2 and 3.4, respectively.

In this paper, we have analyzed the dependence of the activation state of the ATP synthase upon the membrane potential and ΔpH with dark-adapted or pre-illuminated leaves by measuring the kinetics of membrane potential decay following pulses of saturating light. On this basis, we propose a new method to estimate the $\Delta\tilde{\mu}_{H^+}$ level that is in equilibrium with the phosphate potential in the dark.

* Corresponding author. Tel.: +33 1 58 41 50 44.
E-mail address: pjoliot@ibpc.fr (P. Joliot).

0005-2728/$ – see front matter © 2008 Elsevier B.V. All rights reserved.
doi:10.1016/j.bbabio.2008.04.010

2. Materials and methods

Experiments were performed with young spinach leaves. When stated, the leaf was infiltrated under low pressure with 0.15 M sorbitol. During experiments, humid air was continuously flowed to the leaf.

Spectrophotometric and fluorescence measurements were performed using a new spectrophotometer (Biologic Science Instruments JTS10) in which absorption changes are sampled by weak monochromatic flashes (10-nm bandwidth) provided by light-emitting diodes (LED). The time resolution of the method is equal to the duration of the detecting flashes (12 μs). Continuous illumination was provided by LEDs peaking at 630 nm. Saturating actinic flashes were provided by a dye laser (630 nm) pumped by the second harmonic of a Nd Yag laser (6-ns total duration). Membrane potential changes were measured by the difference of absorption (520 nm–546 nm). This difference eliminates the contributions of P_{700} and scattering changes. Owing to the low noise level of the method ($\Delta I/I \sim 10^{-5}$), a single experiment was performed at each wavelength. The extent of the field-indicating changes measured at 520 nm is proportional to the transmembrane electrical potential (reviewed in [18]). It has been explained on the grounds of a strong pre-existing polarization of the pigment probes. We have previously shown [19] that, in young spinach leaves, the concentration of PSII and PSI centers is about equal so that the absorption change measured 100 μs after a short saturating flash is proportional to the membrane potential increase associated with the transfer of two charges per photosynthetic chain. Membrane potential changes were calibrated with respect to the membrane potential changes induced by a single charge separation per photosynthetic chain (1 r. u.) that is typically equal to $\Delta I/I \sim 3\times10^{-3}$ and $\sim 2.2\times10^{-3}$ for non-infiltrated and infiltrated leaf, respectively.

The intensity of the continuous illumination was calibrated by measuring, with a dark-adapted leaf, the initial rate R_i of the membrane potential increase, expressed in r. u./s. Assuming that the actinic light (630 nm) excites equally PSI and PSII, the photochemical rate constant, expressed as the number of photons trapped by a photochemical center per second, is: $ki_{PSI} \sim ki_{PSII} \sim R_i/2$.

In this paper, the absolute value of the membrane potential and of the electrochemical proton gradient are noted as $\Delta\varphi$ and $\Delta\tilde{\mu}_{H^+}$, respectively. When measured with respect to the dark-adapted levels $\Delta\varphi_{dark}$ and $\Delta\tilde{\mu}_{H^+dark}$, the $\Delta\varphi$ and $\Delta\tilde{\mu}_{H^+}$ changes induced by an illumination are noted $\Delta\Delta\varphi$ and $\Delta\Delta\tilde{\mu}_{H^+}$, respectively. Thus, the absolute value of the membrane potential is $\Delta\varphi = \Delta\varphi_{dark} + \Delta\Delta\varphi$.

The photochemical rate (R_{PSII}) is computed by measuring the fluorescence yield that is linearly related to R_{PSII}. If F is the fluorescence yield measured at a given time after the onset of a continuous illumination and F_{max} the maximum fluorescence yield measured after a superimposed pulse of saturating light, R_{PSII} is given by the ratio $(F_{max}-F)/F_{max}$ [20].

3. Results and discussion

3.1. Membrane potential changes induced by saturating light-pulses

In Fig. 1A, the light-induced membrane potential change has been measured with a dark-adapted leaf submitted to a single pulse of strong light with various intensities. The duration of the pulse was such that the maximum membrane potential level was reached, and the time at which the light was switched off was taken as time zero. For $ki_{PSI} \sim ki_{PSII}$ ~7000, 670 and 330 s^{-1}, the values of the membrane potential increase ($\Delta\Delta\varphi_{max}$) reached after ~8, ~13 and ~18 ms, respectively, increased with the light intensity. The polyphasic decay of the membrane potential analyzed over the first 20 ms (linear scale) and over a period of 10 s (log scale) are shown in Fig. 1B and C, respectively. The decay kinetics displays a first phase (phase 1), completed in ~15 ms ($t_{1/2}$ ~2.6 ms), the amplitude of which increases with the light intensity. Beyond 15 ms, the membrane potential decay is independent of the light intensity. It suggests that phase 1 reflects a different process than the subsequent ones. Kinetics of fluorescence increase measured on a leaf submitted to high-light illumination shows that the time required to fully reduce the plastoquinone (PQ) pool and the PSI acceptors (~40 and ~200 ms, respectively [21,22]) is much longer than the duration of the pulse used for curve 1 (8 ms). We thus propose that phase 1 (Fig. 1B) is associated with rapid ion transfers across the membrane that is triggered above a threshold level of the membrane potential rather than from a decrease in the rate of membrane potential generation. The threshold potential, $\Delta\Delta\varphi_{leak}$ that is determined by the extrapolation to time zero of the second phase of the decay kinetics (Fig. 1B, arrow) is independent of the light intensity ($\Delta\Delta\varphi_{leak} \sim 5.5$ r. u.). The origin of the rapid ion transfers triggered above $\Delta\Delta\varphi_{leak}$ will be discussed in Section3.7.

3.2. Determination of the membrane potential in dark-adapted leaves and light-induced activation of ATP synthase

As a working hypothesis, we consider that the $\Delta\varphi_{leak}$ level characterized in Section 3.1 provides a reference level for the transmembrane potential. In order to test the validity of this hypothesis, one must estimate the membrane potential that may pre-exist in the dark $\Delta\varphi_{dark}$ to which $\Delta\Delta\varphi_{leak}$ would be superimposed.

The rate of charge recombination between PSII acceptor and donor measured in thylakoids in the presence of 3-(3,4-dichloro-phenyl)-1,1-dimethylurea (DCMU) is known to increase with both the membrane potential and the proton gradient [23–25]. The kinetics of fluorescence decay induced by short flashes has been measured with dark-adapted Chlorella cells in the presence of DCMU [3]. The half time for the reoxidation of Q_A^- is increased by a factor of ~2 upon addition of tri-butyl-tin, a specific inhibitor of ATP synthase. This was interpreted by assuming that a pool of ATP is present in the chloroplasts, the hydrolysis

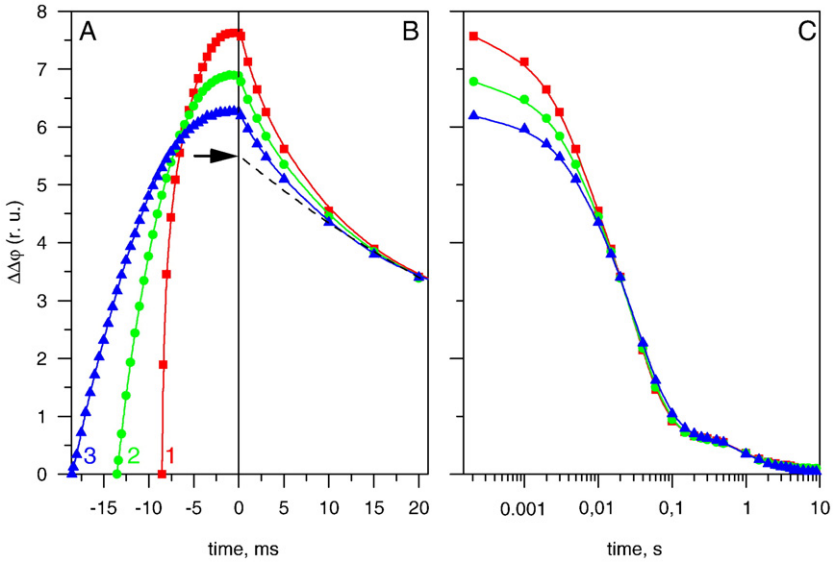

Fig. 1. Light-induced membrane potential changes for different light intensities. $ki_{PSI} \sim ki_{PSII} \sim 7000$, ~670 and ~330 s^{-1} for curves 1–3, respectively. The leaf is dark-adapted for more than 2 h. A: Membrane potential increase measured during the light-pulse. B: Membrane potential decay measured from 0 to 20 ms (linear scale) after the light-pulse. Dashed line: Membrane potential decay after subtraction of phase 1; arrow: $\Delta\varphi_{leak} \sim 5.5$ r. u. C: Membrane potential decay measured from 10 μs to 10 s (logarithmic scale).

of which induces a permanent electrochemical proton gradient. Bennoun [6] demonstrated that, in aerobic conditions, this pool of ATP is of mitochondrial origin. We performed similar experiments with leaves and measured the fluorescence decay following a 10-ns flash in the presence of 20-μM DCMU. In order to get fluorescence changes roughly proportional to Q_a^-, we used non-saturating flashes hitting ~20% of PSII centers [3,26]. The half times of the fluorescence decay were ~1.1 s in the control and ~2.5 s in the presence of a saturating concentration of uncouplers (2-μM nigericin+2-μM nonactin) that fully collapses the $\Delta\tilde{\mu}_{H^+}$ pre-existing in the dark. This dependence of the rate of charge recombination on the addition of uncouplers shows that a membrane potential, likely associated with ATP hydrolysis, is present in dark-adapted leaves, as previously observed in algae [3]. To test the mitochondrial origin of the ATP pool accounting for this $\Delta\tilde{\mu}_{H^+}$, we repeated the above experiment in the presence of antimycin, an inhibitor of the cyt *b*/*c* complex of the respiratory chain. The half times of the fluorescence decay measured in the presence of 5-μM and 40-μM antimycin were ~2.06 and ~2.53 s, respectively. Thus, the addition of 40-μM antimycin, as well as saturating concentration of uncouplers fully collapses $\Delta\varphi$ and $\Delta\tilde{\mu}_{H^+}$. It proves that, in the dark-adapted chloroplasts, ATP is of mitochondrial origin.

If indeed a $\Delta\varphi$ component is present in the dark, the light-induced $\Delta\Delta\varphi$ measured in Fig. 1 is superimposed to a "pedestal", which can be collapsed by addition of antimycin. In Fig. 2, we measured the effect of antimycin on the kinetics of the membrane potential increase induced by a pulse of strong light ($ki_{PSI} \sim ki_{PSII} \sim 5000\ s^{-1}$) given to a dark-adapted leaf. As shown in Fig. 2A, $\Delta\Delta\varphi_{max}$ is larger in the presence of antimycin than in its absence. These differences in $\Delta\Delta\varphi_{max}$ do not reflect changes in the rate of charge separation (see equal initial slopes for curves 1–3, Fig. 2A) but rather witness the decrease of the pedestal since we have shown that addition of antimycin collapses $\Delta\varphi_{dark}$. Accordingly, we propose that $\Delta\varphi_{max} = \Delta\varphi_{dark} + \Delta\Delta\varphi_{max}$. Moreover, as just discussed, in the presence of 40-μM antimycin (Fig. 2A, curve 4) we have $\Delta\varphi_{dark} = 0$. In Fig. 2B, we have plotted curves 1–4 assuming equal $\Delta\varphi_{max}$ value. This allows the determination of $\Delta\varphi_{dark}$ in the absence of antimycin, which is equal to 3.6 r. u. (dashed line 1) and suggests that the addition of increasing concentration of antimycin results in a decrease of $\Delta\varphi_{dark}$ owing to a decrease of ATP concentration.

Previous reports showed that the membrane potential decay measured after the illumination of thylakoids [14] or leaf [16] by a series of short flashes displays a biphasic kinetics. The first phase completed in ~100 ms has been ascribed to proton transfer through ATP synthase that is associated with ATP synthesis and the slower phase, completed in ~1 s, to ions leaks through the membrane. The break between the two phases has been interpreted as reflecting the switch of the ATP synthase from an active to an inactive state that occurs below a threshold level of the membrane potential [14].

Fig. 2C shows the multiphasic decay of the membrane potential measured after the light is switched off. The first phase completed in ~15 ms we ascribe to rapid ion transfers through the membrane (Section 3.1) has not been observed in [15,16]. In these experiments, thylakoids or leaves were submitted to a series of short saturating flashes that induces a lower membrane potential increase than that induced by a pulse of saturating light as we used in Figs. 1 and 2. The lack of phase 1 in the decay kinetics reported in [15,16] is explained by the fact that the flash-induced membrane potential increase is lower than $\Delta\varphi_{leak}$.

Decay kinetics shown Fig. 2C display a second phase (phase 2, completed in 100 ms) of equal amplitude for curves 1 to 4. In agreement with [14], we assume that this phase, is associated with proton transfer that leads to ATP synthesis. Interestingly, the extrapolation to time zero of phase 3, completed in 2 s, leads to an equal value of $\Delta\varphi_{thr}$ level for curves 1–4 ($\Delta\varphi_{thr} \sim 5.9$ r. u.). Thus, we now define 3 membrane potential reference levels that do not depend upon antimycin concentration: $\Delta\varphi_{max} \sim 11.6$ r. u., $\Delta\varphi_{leak} \sim 9.2$ r. u. and $\Delta\varphi_{thr} \sim 5.9$ r. u.

In Fig. 2C, curves 1–3 (dashed lines), the permanent membrane potential $\Delta\varphi_{dark}$ is lower than $\Delta\varphi_{thr}$ but not null. It shows that, below $\Delta\varphi_{thr}$, ATP synthase remains able to slowly hydrolyze ATP and thus, able to generate a permanent membrane potential in contradiction with the conclusion drawn in [14]. Phase 3 is followed by phase 4, completed in 1 to 2 min, which we ascribe to the slow metabolic consumption of the ATP that has been synthesized during and after the pulse of saturating light. It should be kept in mind that under the conditions of the present experiments (i.e. dark-adapted leaves), the Benson–Calvin cycle is not activated so that the pool of ATP is not engaged into CO_2 fixation. We propose that 5 μM-antimycin inhibits

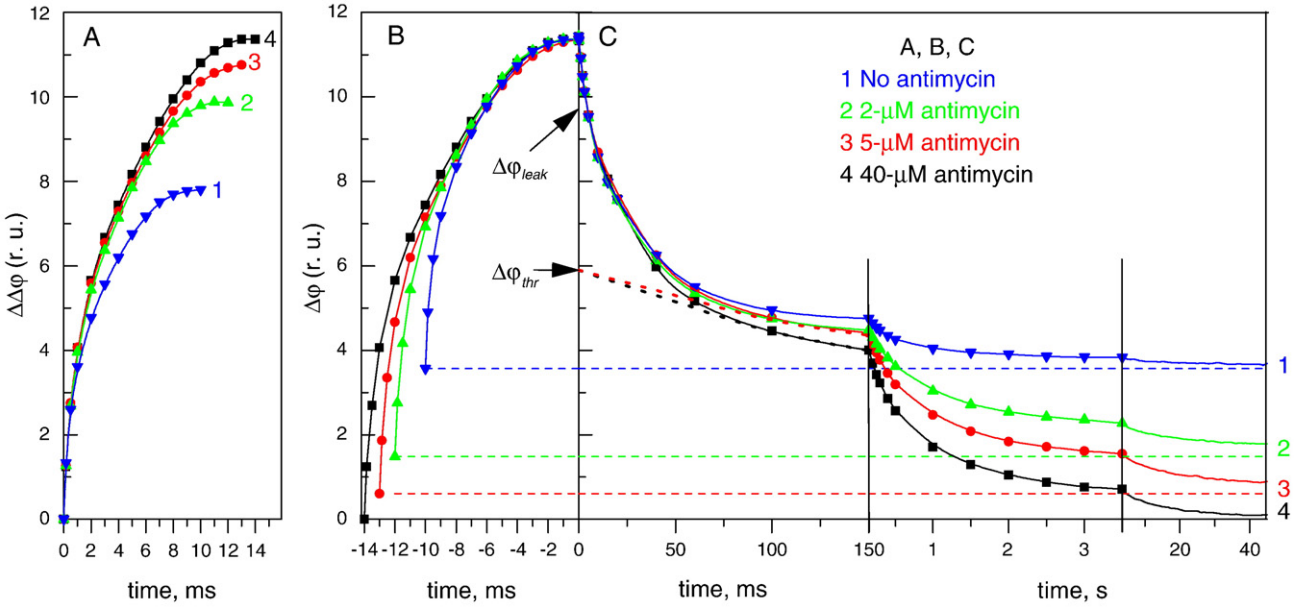

Fig. 2. Light-induced membrane potential changes in the presence or absence of antimycin. A. Membrane potential increase measured during light-pulses ($ki_{PSI} \sim ki_{PSII} \sim 5000\ s^{-1}$) given to dark-adapted leaves. The leaf is infiltrated with 0.15 M sorbitol. Curve 1, control. Curves 2–4, 2-μM, 5-μM and 40-μM antimycin, respectively. B. Curves 1–4 as in panel A but plotted assuming an equal value for $\Delta\varphi_{max}$. Dashed lines, $\Delta\varphi_{dark}$ levels for curves 1–3. C. Membrane potential decay measured after the light-pulses.

cyt *b*/*c* complexes but that the electron flow via complex I and alternative quinol-oxidases maintains a low level of ATP in the dark. Interestingly, the half time of phase 4 measured in the presence of 40-μM antimycin (~10 s), is significantly shorter than that measured in the presence of 2- and 5-μM antimycin (~22 s). This acceleration suggests that antimycin has a low uncoupling activity able to fully collapse $\Delta\varphi$. Consistent with this hypothesis, the addition of saturating concentrations of other inhibitors of the respiratory chains as myxothiazol (inhibitor of the cyt b/c complex), or KCN (inhibitors of the cytochrome oxidase) induces similar effect than 5-μM antimycin (not shown).

The membrane potential change induced by a single-turnover flash that induces the transfer across the membrane of two charges per photosynthetic chain has been estimated to ~40 mV [18,27,28] (1 r. u. ~20 mV). In the following, we have used this value to calibrate membrane potential changes. In the presence of 40-μM antimycin (Fig. 2B, curve 4), we have $\Delta\varphi_{max}$ ~11.5 r. u. and $\Delta\varphi_{leak}$ ~9.6 r. u., which corresponds to ~230 and ~192 mV, respectively. These values are in reasonable agreement with the estimate of the maximum potential an artificial or biological membrane can sustain (~200 mV, [29,30]. Further, we have $\Delta\varphi_{thr}$ ~5.9×20 ~98 mV and $\Delta\varphi_{dark}$ ~3.7×20 ~74 mV (dashed line 1, Fig. 2B).

3.3. Equivalence of chemical and electrical potential for the activation of ATP synthase

In the following, we will attempt to address the question as to whether the threshold levels for ATP synthase activity and for ion leaks depend exclusively on $\Delta\varphi$ or rather on the electrochemical proton gradient $\Delta\tilde{\mu}_{H^+}$. We quote the chemical potential associated with ΔpH as $\Delta\tilde{\mu}_{pH}$=0.06 ΔpH and we have $\Delta\tilde{\mu}_{H^+}=\Delta\varphi+\Delta\tilde{\mu}_{pH}$.

In Fig. 3A, the leaf has been infiltrated with 0.6-μM nigericin to rapidly convert ΔpH into $\Delta\varphi$. Addition of nigericin induces a decrease in $\Delta\Delta\varphi_{max}$, and thus in $\Delta\varphi_{dark}$ levels (not shown). Curve 1 shows the kinetics of the membrane potential decay measured after a 12-ms light-pulse given to a dark-adapted leaf. In a second experiment, the same leaf has been first illuminated by a 200-ms light-pulse that induces a $\Delta\varphi$ increase that decays in several minutes ($t1/2$ ~1 min). We assume that $\Delta\varphi$ is in thermodynamic equilibrium with the phosphate potential for time longer than 10 s. It implies that the $\Delta\varphi$ decay is associated with the metabolic consumption of the ATP synthesized during the 200-ms light-pulse. In Fig. 3A, the red arrow indicates the membrane potential measured 26 s after the 200-ms pulse ($\Delta\Delta\varphi$ ~1.31). Curve 2 shows the membrane potential decay measured after a 12-ms light-pulse given 26 s after the 200-ms pulse. Fig. 3A insert shows that the initial rate of the membrane potential decay and the amplitude of phase 1 are lower with the pre-illuminated leaf (curve 2) than with the dark-adapted leaf (curve 1). It implies that the rate of the charge separation at the end of the 12-ms light-pulse is lower for curve 2 than for curve 1. We have previously shown [18] that a large fraction of the PQ pool is still reduced 26 s after the 200-ms light-pulse. Thus, one expects that, at end of the 12-ms pulse, PSII turnover and the rate of charge separation are slower for curve 2 than for curve 1, which explains the lower amplitude of phase 1. Beyond 15-ms dark, curves 1 and 2 are identical, as are curves 1–3 of Fig. 1B. Consequently, both $\Delta\Delta\varphi_{leak}$ (~8 r. u) and $\Delta\Delta\varphi_{thr}$ (~4.35) are the same for curves 1 and 2, Fig. 3A. We have checked that for dark times longer than 26 s between the 12-ms and the 200-ms light-pulses, phase 2 remains identical to that measured with the dark-adapted material.

Fig. 3B shows the same experiment as Fig. 3A but performed in the absence of nigericin and in the presence of 3-μM antimycin. Antimycin concentration was adjusted to get the same $\Delta\Delta\varphi_{max}$ level that measured in the presence of nigericin (Fig. 3A and B, curves 1). The membrane potential measured 26 s after the 200-ms pulse ($\Delta\Delta\varphi$ ~0.67, Fig. 3B, red arrow) is about half than that measured in the presence of nigericin (~1.31), suggesting that the $\Delta\tilde{\mu}_{pH}$ component in the dark is not null. Moreover, contrary to what is observed in the presence of nigericin, curve 2 (pre-illuminated leaf) is shifted toward lower membrane potential values with respect to curve 1 (dark-adapted leaf). This downshift (0.64 r. u.) is consistent with the following hypotheses: 1) in the absence of nigericin, the hydrolysis of ATP generated by the 200-ms pulse induces the formation of a proton gradient superimposed to a membrane potential increase; 2) the threshold level for ATP synthase activity is set by the electrochemical proton gradient rather than by the sole membrane potential; and 3) in the presence of either nigericin or antimycin, the 200-ms light-pulse induces the synthesis of the same amount of ATP that is associated with the same increase in the electrochemical proton gradient. In the presence of nigericin, we have: $\Delta\Delta\tilde{\mu}_{H^+}=\Delta\Delta\varphi$=~1.31 r. u. In the presence of antimycin, $\Delta\Delta\tilde{\mu}_{H^+}$ is the sum of a proton gradient $\Delta\Delta\tilde{\mu}_{pH}$ ~0.64 r. u. equal to the downshift between curves 1 and 2, Fig. 3B and of the membrane potential $\Delta\Delta\varphi$=~0.67 r. u. measured 26 s

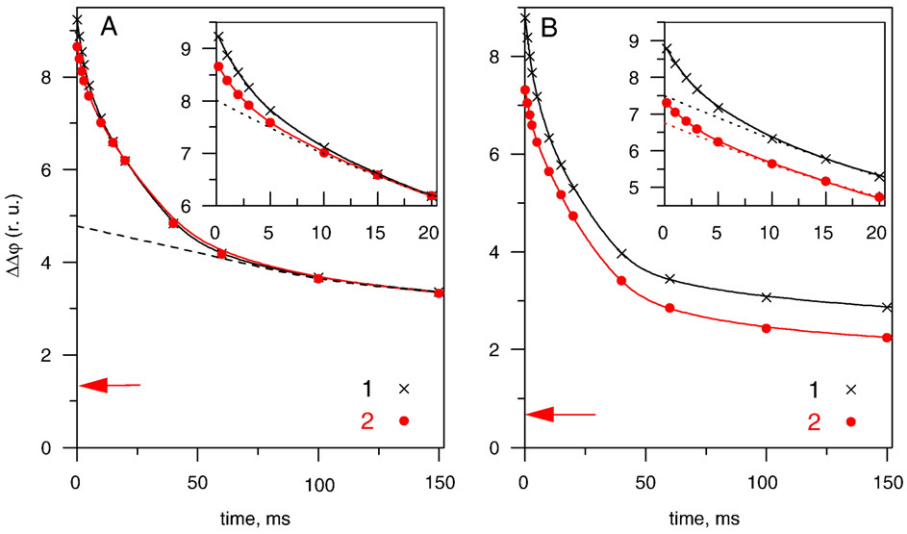

Fig. 3. Effect of nigericin on the membrane potential decay measured after light-pulses. A. The leaf is infiltrated with 0.15 M sorbitol+0.6 μM nigericin. Curve 1, (×) membrane potential decay measured after illumination by a 12-ms light-pulse (ki_{PSI} ~ ki_{PSII} ~5000 s^{-1}) given to a dark-adapted leaf. Curve 2, (●) membrane potential decay measured after a 12-ms light-pulse given 26-s after a 200-ms light-pulse (same intensity of illumination for both pulses). Red arrow: membrane potential level measured 26-s after the 200-ms light-pulse (1.31 r. u.). A, insert: As A but plotted with expended time scales. B: The leaf is infiltrated with 0.15 M sorbitol and 3-μM antimycin. Same program of illumination and same symbols as in A. Red arrow: Membrane potential level measured 26-s after the 200-ms light-pulse (0.67 r. u.).

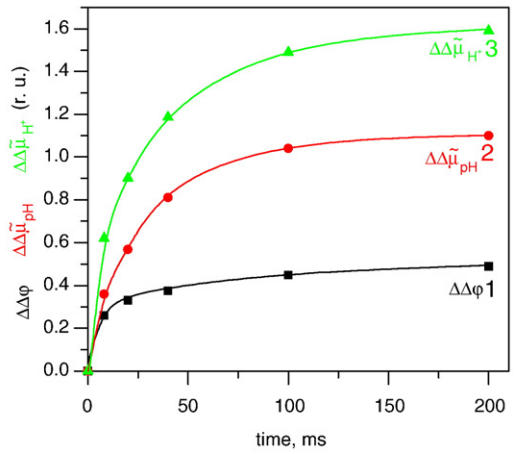

Fig. 4. $\Delta\Delta\varphi$, $\Delta\Delta\tilde{\mu}_{pH}$ and $\Delta\Delta\tilde{\mu}_{H^+}$ induced by light-pulses of different duration. Intensity of illumination: $ki_{PSI} \sim ki_{PSII} \sim 5000\ s^{-1}$. The leaf is illuminated by a first pulse (duration 8 to 200-ms). A second light-pulse (11-ms) is given 30-s after the first one. $\Delta\Delta\varphi$, $\Delta\Delta\tilde{\mu}_{pH}$ and $\Delta\Delta\tilde{\mu}_{H^+}$ are computed using the same procedure as in Fig. 3B and are plotted as a function of the duration of the first pulse.

after the 200-ms pulse is given. It leads to $\Delta\Delta\tilde{\mu}_{H^+} \sim 0.64 + \sim 0.67 \sim 1.31$ r. u., a value equal to that measured in the presence of nigericin, in agreement with hypothesis 3. Since $\Delta\Delta\varphi_{thr}$ and $\Delta\Delta\varphi_{leak}$ undergo similar downshifts after the 200-ms light-pulse (Fig. 3B and insert), we conclude that the threshold levels for ion leaks and for ATP synthase activity are both controlled by the electrochemical proton gradient.

We have proposed that the long-lived $\Delta\tilde{\mu}_{H^+}$ increase induced by the 200-ms light-pulse reflects the light-induced increase in ATP concentration. In Fig. 4, using the same procedure as in Fig. 3, we have measured $\Delta\tilde{\mu}_{H^+}$ increase as a function of the duration of the light-pulse. As just discussed, $\Delta\Delta\varphi$ was measured 30-s after the illumination and $\Delta\Delta\tilde{\mu}_{pH}$ by measuring the downshifts of $\Delta\Delta\varphi_{thr}$ and $\Delta\Delta\varphi_{leak}$. In Fig. 4, curves 1–3 display $\Delta\Delta\varphi$, $\Delta\Delta\tilde{\mu}_{pH}$ and $\Delta\Delta\tilde{\mu}_{H^+}$, respectively, as a function of the light-pulse duration. $\Delta\Delta\tilde{\mu}_{H^+}$ displays a multi phasic kinetics with a first phase completed in 40–50 ms, followed by a ~200-ms phase. This kinetics presents similarity with the multiphasic fluorescence increase induced by a high-light illumination of a dark-adapted leaf [21,31] denoted phases OJIP [32,33]. The OJ and JI phases, completed in ~40 ms [21,31–33], were associated with the reduction of most of the PSII electron acceptors whereas the IP phase, completed in ~200 ms, was ascribed to the reduction of PSI electron acceptors [22]. Thus, the kinetics of fluorescence and $\Delta\tilde{\mu}_{H^+}$ increase both reflect the number of charges transferred through the membrane which is roughly proportional to the number of ATP synthesized.

3.4. Life-time of the light-induced electrochemical proton gradient

In Fig. 5, the decay of $\Delta\Delta\tilde{\mu}_{H^+}$ induced by a 12-s illumination has been measured, using a similar procedure as in Fig. 2. In Fig. 5A, the black curve displays the kinetics of $\Delta\Delta\tilde{\mu}_{H^+}$ increase induced by a 12-ms pulse given to a leaf dark-adapted for more than 3 h. Following a 12-s illumination, short pulses are given at dark times as indicated on Fig. 5. The duration of each of the light-pulses has been adjusted to reach the maximum level $\Delta\Delta\tilde{\mu}_{H^+max}$. Owing to the small number of charges transferred and to the high-buffering capacitance of the lumen, we assume that, during each of these short light-pulses, $\Delta\Delta\tilde{\mu}_{H^+}$ closely reflects $\Delta\Delta\varphi$. The first pulse is given after 45-s dark, a time sufficient to allow the full oxidation of the PSI acceptors and a partial oxidation of the PQ pool. Fig. 5B shows the kinetics of $\Delta\Delta\tilde{\mu}_{H^+}$ decay measured after each pulse. Curves 1–8 display a first phase completed in ~15 ms (phase 1). As already discussed (Section 3.3), both the initial decay rate and the amplitude of phase 1 are lower for the shorter dark periods owing to the fact that the PQ pool is still partially reduced. Solid lines in Fig. 5B display the initial part of phase 2 after subtraction of phase 1. As in Figs. 1–3, $\Delta\Delta\tilde{\mu}_{H^+leak}$ level is estimated by extrapolation to time zero of phase 2.

The data shown in Fig. 2 evidenced that addition of antimycin induced a $\Delta\Delta\tilde{\mu}_{H^+max}$ increase that reflects a decrease of the $\Delta\tilde{\mu}_{H^+dark}$ pedestal. We thus assume that in Fig. 5B, the lower $\Delta\Delta\tilde{\mu}_{H^+max}$ and $\Delta\Delta\tilde{\mu}_{H^+leak}$ levels reflect a larger $\Delta\tilde{\mu}_{H^+}$ pedestal. In Fig. 5C, we have plotted for each of the probing pulses the kinetics of $\Delta\tilde{\mu}_{H^+}$ decay after subtraction of phase 1 assuming equal value for $\Delta\tilde{\mu}_{H^+leak}$ as determined in Fig. 5B. As the $\Delta\tilde{\mu}_{H^+dark}$ pedestal is not known, we have plotted the difference $\Delta\tilde{\mu}_{H^+} - \Delta\tilde{\mu}_{H^+dark}$. Dashed lines show the $(\Delta\tilde{\mu}_{H^+} - \Delta\tilde{\mu}_{H^+dark})$ level measured at the times each of the probing pulses is given. This level decreases when the dark time increases. We ascribe the light-induced $\Delta\tilde{\mu}_{H^+}$ increase to the ATP synthesis induced by the efficient cyclic electron flow that operates during the 12-s illumination [19,34]. During the subsequent dark period, $\Delta\tilde{\mu}_{H^+}$ and ATP concentration slowly decrease to their dark-adapted values. For dark times longer than 15-min, the amplitude and time-course of phase 2 stay constant while the amplitude of phase 3 (completed in 4-s) increases with the time of dark adaptation. Thus, beyond 15-min dark

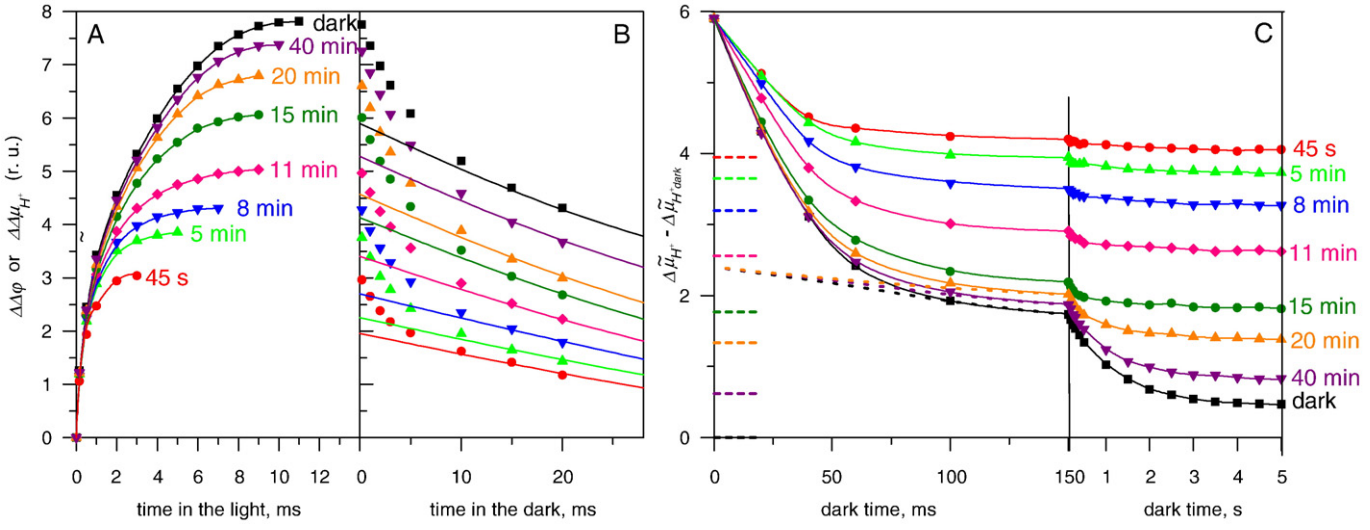

Fig. 5. Electrochemical proton gradient induced by a short light-pulse ($ki_{PSI} \sim ki_{PSII} \sim 5000\ s^{-1}$) given at various dark times after a 12-s illumination ($ki_{PSI} \sim ki_{PSII} \sim 400\ s^{-1}$). Dark times as indicated in panels A and C. A: $\Delta\Delta\tilde{\mu}_{H^+}$ increase measured during the short light-pulse. B: $\Delta\Delta\tilde{\mu}_{H^+}$ decay measured after the short light-pulse. Solid lines: phase 2 (see text). C: $\Delta\tilde{\mu}_{H^+} - \Delta\tilde{\mu}_{H^+dark}$ decay kinetics (phases 2 and 3) measured after the short light-pulses plotted assuming the same value for $\Delta\tilde{\mu}_{H^+leak}$. Dashed lines: $\Delta\tilde{\mu}_{H^+} - \Delta\tilde{\mu}_{H^+dark}$ measured at the time the short light-pulses are given. Dotted lines: extrapolation to time zero of phase 3, giving the threshold level for ATPase activation ($\Delta\tilde{\mu}_{H^+thr} - \Delta\tilde{\mu}_{H^+dark} \sim 2.4$ r. u.).

time, the curves display equal threshold level for ATP synthase activation ($\Delta\tilde{\mu}_{H^+thr} - \Delta\tilde{\mu}_{H^+dark}$ ~2.4). For dark times up to 15-min, $\Delta\tilde{\mu}_{H^+} - \Delta\tilde{\mu}_{H^+dark}$ measured at the time the probing pulses are given is larger than $\Delta\tilde{\mu}_{H^+thr}$. Under these conditions, ATP synthase is already in its activated state at the time the light-pulse is given and most of the $\Delta\tilde{\mu}_{H^+}$ decay is completed in ~100 ms (phase 2). At the time the first probing pulse is given (45 s after the 12-s illumination), we have $\Delta\tilde{\mu}_{H^+} - \Delta\tilde{\mu}_{H^+thr}$ ~1.5 r. u. According to Fig. 2C, the absolute $\Delta\tilde{\mu}_{H^+thr}$ level is ~5.9 r. u. Thus, in Fig. 5, the absolute $\Delta\tilde{\mu}_{H^+}$ level measured 45 s after the 12-s illumination is $\Delta\tilde{\mu}_{H^+}$ ~1.5+~5.9=~7.4 r. u.=~150 mV.

In Fig. 6, $\Delta\tilde{\mu}_{H^+} - \Delta\tilde{\mu}_{H^+dark}$ decay has been measured as a function of the dark time following an illumination by giving a series of probing pulses as previously described (Fig. 5C, dashed lines). Curves 1–3 show the $\Delta\tilde{\mu}_{H^+} - \Delta\tilde{\mu}_{H^+dark}$ decay after 6-s, 30-s and 10-min illumination, respectively. The extrapolation to time zero of curves 1–2 is $\Delta\tilde{\mu}_{H^+} - \Delta\tilde{\mu}_{H^+dark}$ ~4.1 r. u., a value close to that measured in Fig. 5C after 45-s dark (3.9 r. u.). The same value is obtained for times of illumination from 6-s to 2-min (not shown). In Fig. 6, curve 3, the time of illumination (10-min) is long enough to fully activate the Benson–Calvin cycle. During the first minute in the dark $\Delta\tilde{\mu}_{H^+}$ is slightly lower than that measured in curves 1–2. It may reflect a lower ATP concentration owing to its fast consumption by the Benson–Calvin cycle. Curves 1–3 display a lag phase, the duration of which increases with the time of illumination. This lag phase can be tentatively ascribed to the buffering capacitance associated with the storage of high-energy phosphate bounds present in the numerous compounds, the synthesis of which are coupled to ATP hydrolysis including those involved in the Benson and Calvin cycle. The $\Delta\tilde{\mu}_{H^+} - \Delta\tilde{\mu}_{H^+dark}$ decay that follows the lag phase displays two phases completed in ~15 min and >1 h. The amplitude of the slower phase increases as a function of the time of illumination to reach a maximum value after ~10 min (Fig. 6, curve 3, ~25% of the total amplitude). This phase could reflect a slow equilibration between the chloroplast and the cytoplasm compartments.

3.5. Control of the activity of the Benson–Calvin cycle by ATP

Three molecules of ATP and two molecules of NADPH supply the energy and reductive power required for the assimilation of one CO_2 molecule. On the other hand, the activity of several enzymes of the Benson–Calvin cycle is controlled by the light-induced increase of the stromal pH and Mg^{2+} concentration together with the reduction of intramolecular disulfide bounds by a process involving ferredoxin and thioredoxin.

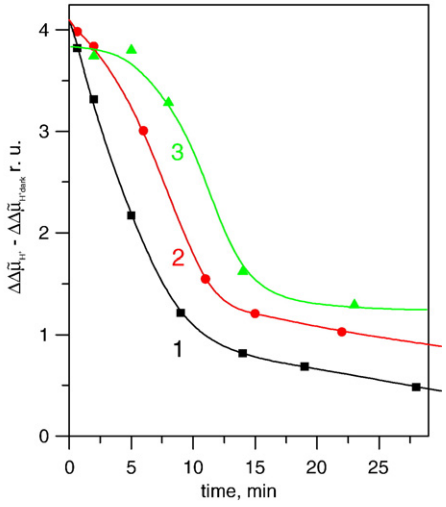

Fig. 6. Light-induced electrochemical proton gradient as a function of the dark time following an illumination ($ki_{PSI} \sim ki_{PSII} \sim 400\ s^{-1}$). $\Delta\tilde{\mu}_{H^+}$ $\Delta\tilde{\mu}_{H^+dark}$ is measured at the time the probing pulses are given according to the method described in Fig. 5C, dashed lines. Curves 1–3: duration of illumination 6-s, 30-s, and >10 min, respectively.

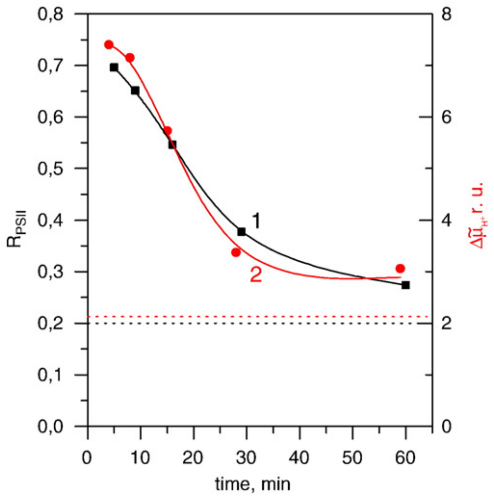

Fig. 7. Deactivation of the Benson–Calvin cycle as a function of the dark time following a 10-min green illumination ($ki_{PSII} \sim 60\ s^{-1}$). Curve 1: R_{PSII} is measured at the end of each of the 1.8-s illuminations given at times indicated by the black points. R_{PSII} is computed according to Genty formula (see Materials and methods). Black dotted line: R_{PSII} measured with the leaf dark-adapted for more than 2 h. Curve 2: $\Delta\tilde{\mu}_{H^+}$ as a function of the dark time following the 10-min illumination measured according to the method described in Fig. 5C. Red dotted line: $\Delta\tilde{\mu}_{H^+dark}$ estimated on the basis of an experiment performed in the presence of 40-μM antimycin (see Fig. 2).

In Fig. 7, a dark-adapted mature leaf is illuminated for 10-min of moderate light ($ki_{PSII} \sim 60\ s^{-1}$). The rate of the Benson–Calvin cycle then is probed by 1.8-s illuminations, given at various dark times following the 10-min illumination. At the end of each of these 1.8-s illuminations, the electron flow through the membrane-bound photosynthetic chain reaches a quasi-equilibrium state, the rate of which is limited by the rate of NADPH oxidation via the Benson–Calvin cycle. Thus, this rate can be assessed by measuring the rate of any step including the PSII photoreaction. The rate of PSII photoreaction (R_{PSII}) (Fig. 7, curve 1) is measured by fluorescence techniques at the end of the 1.8-s illuminations (see Materials and methods). Fig. 7, curve 2 displays $\Delta\tilde{\mu}_{H^+}$ measured with the same leaf as a function of the dark time following the 10-min illumination. Decays of R_{PSII} and $\Delta\tilde{\mu}_{H^+}$ display similar time-course with a first phase completed in ~20 min and a second phase that lasts for more than 1 h. This experiment suggests that, in a mature leaf, the rate of the Benson–Calvin cycle is mainly controlled by ATP concentration. The absence of a deactivation phase in a few min time range suggest that the redox-regulated enzymes of the Benson–Calvin cycle are in their reduced (active) state in dark-adapted and pre-illuminated leaves as well. In the presence of 10-μM myxothiazol, all the cell compartments are deprived in ATP and we observed that short periods of illumination (<30-s) induce no long-lived $\Delta\tilde{\mu}_{H^+}$ increase (not shown). It suggests that in these conditions, ATP synthesized by the cyclic electron flow is rapidly consumed in the different cell compartments that lack ATP.

3.6. Phosphate potential and ATP concentration

If one assumes that the membrane is in thermodynamic equilibrium, we have:

$$\Delta\tilde{\mu}_{H^+} = 60/n \times (\log K + \log (R/[P])) \quad (1)$$

in which R is equal to the [ATP]/[ADP] ratio, n is the number of protons translocated through the ATP synthase per ATP synthesized and $\Delta\tilde{\mu}_{H^+}$ is expressed in mV. According to Turina et al. [35], the H^+/ATP ratio is n=4. From the value of the Gibbs free energy for ATP synthesis [35,36] and assuming a stromal pH between 7 and 8, we estimate $K \sim 2 \times 10^5$. On this basis, we have:

$$\Delta\tilde{\mu}_{H^+} = 80 + 15 \times \log R/[P]. \quad (2)$$

As computed from Fig. 5, $\Delta\tilde{\mu}_{H^+}$ level measured 45 s after the 12-s illumination is ~150 mV, that leads to $R/[P]$~34000. If the membrane is in thermodynamic equilibrium and assuming $[P]$~1 mM, it would correspond to a large [ATP]/[ADP] ratio (R~45). It suggests that, when a leaf is illuminated for more than 5-s, most of the ADP has been converted to ATP. Generation of ATP is associated with an efficient cyclic process that is operating during the first min of illumination of a dark-adapted leaf [19,34].

In a dark-adapted leaf (Fig. 2C, curve 1), $\Delta\tilde{\mu}_{H^+dark}$ has been estimated to ~74 mV. Depending upon the physiological state of the leaf, $\Delta\tilde{\mu}_{H^+dark}$ varies between 30 mV and 80 mV. For $\Delta\tilde{\mu}_{H^+dark}$~50 mV, we have: $R/[P]$=~10^{-2}, which corresponds to [ATP]/[ADP]=~5×10^{-5} assuming $[P]$=~5 mM. One expects that, at such a low ATP concentration and under conditions in which ATP synthase is mainly inactivated, Eq. (2) is not satisfied owing to passive ion leaks. It suggests that, in dark-adapted leaves, ATP concentration is larger than that computed from Eq. (2).

3.7. Origin of rapid ion transfers associated with phase 1

As shown in Sections 1 and 2, rapid ion transfers are triggered above a membrane potential level $\Delta\varphi_{leak}$~9.6 r. u. equivalent to ~190 mV. The origin of these fast ion transfers is presently unknown. A first possibility is that these ion transfers occur via specific membrane channels, the opening of which would be triggered above a given membrane potential. As an alternative hypothesis, one may assume that, beyond this membrane potential level, the rate of ATP synthesis at the level of the F_1 complex has reached its maximum value likely limited by the rate of the rotation of the electrical rotor F_0 still increases (proton slip). A third hypothesis is to assume that phase 1 and phase 2 are both coupled to ATP synthesis. It would imply that above $\Delta\varphi_{leak}$, ATP synthase activity suddenly increases and ATP synthase activity would be controlled by two threshold levels. This hypothesis appears quite unlikely.

3.8. Regulation of ATP synthase activity

Junesh and Graber [12] and Strelow and Rumberg [17] have measured in vitro the ΔpH that induces the half activation of reduced ATP synthase. Half activation occurs at ΔpH~2.2 [12] or ΔpH~1.65 [17], that correspond to ~130 mV and ~100 mV respectively, assuming the equivalence between $\Delta\varphi$ and $\Delta\tilde{\mu}_{pH}$. These values are close to our estimate of the threshold level for activation of ATP synthase ($\Delta\tilde{\mu}_{H^+thr}$~5.9×20=~118 mV) but much lower than that measured in vitro for the half activation of oxidized ATP synthase (ΔpH=~3.4, equivalent to ~200 mV [12,17]). We thus propose that, in dark-adapted leaves, the γ-subunits that controls ATP synthase activity are in their reduced (active) form. It agrees with our previous conclusion that the enzymes of the Benson–Calvin cycle are also in their reduced form in dark-adapted leaves (see Section 3.5).

Our interpretation of the light-induced activation of the ATP synthase differs from that proposed by Kramer and Crofts [16] who assume that ATP synthase is in its oxidized form in dark-adapted leaves and that its activation results from the reduction of PSI acceptors in the light. Their interpretation was based on the observation that addition of 3-mM methylviologen, a potent electron acceptor expected to preclude the reduction of the thioredoxin, cancels the light-induced activation of the ATP synthase. Such a redox modulation of ATP synthase activity would not induce changes in $\Delta\tilde{\mu}_{H^+thr}$ level but would change the ratio between the concentration of active (reduced) and inactive (oxidized) ATP synthase that would be associated with changes in the kinetics of phase 2 in contradiction with the experiments shown in Fig. 2, curves 1–4 or Fig. 5, curves 5–8). Effect of methylviologen reported in [16] could be interpreted assuming that the formation of H_2O_2 associated with the reoxidation of methylviologen induces the oxidation of ATP synthase, leading to its transitory inactivation.

A corollary to the presence of a permanent $\Delta\tilde{\mu}_{H^+}$ in dark-adapted leaves is that, below $\Delta\tilde{\mu}_{H^+thr}$, ATP synthase remains partially active, in contradiction with the conclusion drawn in [14]. Since thylakoid membranes are more permeable to ions in vitro than in vivo, we suggest that, in vitro, the slow phase of the membrane potential decay (~300-ms [14]) is mainly associated with passive ion leaks rather than coupled to ATP synthesis. When comparing the half times of the fast and slow phases for $\Delta\tilde{\mu}_{H^+}$ decay (~20-ms and 1-s, respectively), we estimate that the activity of ATP synthase below $\Delta\tilde{\mu}_{H^+thr}$ is, at the least, 50 times lower than in its activated state.

According to Junesh and Gräber [12], the activation of reduced ATP synthase occurs within a large ΔpH range (~1.5 to ~3), equivalent to 90 to 180 mV). It suggests that the fraction of active ATP synthase progressively increases above $\Delta\tilde{\mu}_{H^+thr}$. At variance of [12], Strelow and Rumberg [17] reported that activation of ATP synthase is close to a step function that is completed in ~0.2 ΔpH. In this case, one has to assume that, above $\Delta\tilde{\mu}_{H^+thr}$, ATP synthase suddenly shifts from an inactive to an active form. Further experimental work is required to determine if the process of ATP synthase activation in vivo occurs over a narrow or large range of $\Delta\tilde{\mu}_{H^+}$.

Acknowledgement

The authors thank Fabrice Rappaport for the valuable discussions and great help in the preparation of this manuscript.

References

[1] P. Mitchell, Coupling of phosphorylation to electron and hydrogen transfer by a chemi-osmotic type of mechanism, Nature 191 (1961) 144–148.
[2] A.T. Jagendorf, E. Uribe, ATP formation caused by acid-base transition of spinach chloroplasts, Proc. Natl. Acad. Sci. U. S. A. 55 (1966) 170–177.
[3] P. Joliot, A. Joliot, Dependence of delayed luminescence upon adenosine triphosphatase activity in Chlorella, Plant Physiol. 65 (1980) 691–696.
[4] P. Joliot, A. Joliot, Biochim. Biophys. Acta 975 (1989) 355–360.
[5] G. Finazzi, F. Rappaport, In vivo characterization of the electrochemical proton gradient generated in darkness in green algae and its kinetic effects on cytochrome b_6f turnover, Biochemistry 37 (1998) 9999–10005.
[6] P. Bennoun, Chlororespiration revisited: mitochondrial-plastid interactions in *Chlamydomonas*, Biochim. Biophys. Acta 1186 (1994) 59–66.
[7] C. Carmeli, Y. Lifshitz, Effects of P 1 and ADP on ATPase activity in chloroplasts, Biochim. Biophys. Acta 267 (1972) 86–95.
[8] T. Bakker-Grunwald, K. van Dam, On the mechanism of activation of the ATPase in chloroplasts, Biochim. Biophys. Acta 347 (1974) 290–298.
[9] R.A. Ravizzini, C.S. Andreo, R.H. Vallejos, Sulfhydryl groups in photosynthetic energy conservation. VI. Subunit distribution of sulfhydryl groups and disulfide bonds in chloroplast coupling factor and ATPase activity, Biochim. Biophys. Acta 591 (1980) 135–141.
[10] C.M. Nalin, R.E. McCarty, Role of a disulfide bond in the gamma subunit in activation of the ATPase of chloroplast coupling factor 1, J. Biol. Chem. 259 (1984) 7275–7280.
[11] J. Mills, P. Mitchell, Thiol modulation of the chloroplast proton motive ATPase and its effects on photophosphorylation, Biochim. Biophys. Acta 764 (1984) 93–104.
[12] U. Junesch, P. Gräber, Influence of the redox state and the activation of the chloroplast ATP synthase on proton-transport coupled ATP synthesis/hydrolysis. Biochim. Biophys. Acta 893 (1987) 275–288.
[13] W. Junge, The critical electric potential difference for photophosphorylation, Eur. J. Biochem. 14 (1970) 582–592.
[14] W. Junge, B. Rumberg, H. Schröder, The necessity of an electric potential difference and its use for photophosphorylation in short flash groups, Eur. J. Biochem. 14 (1970) 575–581.
[15] P. Joliot, R. Delosme, Flash-induced 519 nm absorption change in green algae, Biochim. Biophys. Acta 357 (1974) 267–284.
[16] D.M. Kramer, A.R. Crofts, Activation of the chloroplast ATPase measured by the electrochromic change in leaves of intact plants, Biochim. Biophys. Acta 976 (1989) 28–41.
[17] F. Strelow, B. Rumberg, Kinetics and energetics of redox regulation of ATP synthase from chloroplasts, FEBS Lett. 323 (1993) 19–22.
[18] H.T. Witt, Energy conversion in the functional membrane of photosynthesis. Analysis by light pulse and electric pulse methods. The central role of the electric field, Biochim. Biophys. Acta 505 (1979) 355–427.
[19] P. Joliot, A. Joliot, Cyclic electron transfer in plant leaf, Proc. Natl. Acad. Sci. U. S. A. 99 (2002) 10209–10214.
[20] B. Genty, J.-M. Briantais, N.R. Baker, The relationship between the quantum yield of photosynthetic electron transport and quenching of chlorophyll fluorescence, Biochim. Biophys. Acta 990 (1989) 87–92.
[21] R. Delosme, [Study of the induction of fluorescence in green algae and chloroplasts at the onset of an intense illumination], Biochim. Biophys. Acta 143 (1967) 108–128.

[22] G. Schansker, S.Z. Toth, R.J. Strasser, Methylviologen and dibromothymoquinone treatments of pea leaves reveal the role of photosystem I in the Chl a fluorescence rise OJIP, Biochim. Biophys. Acta 1706 (2005) 250–261.
[23] C.D. Miles, A.T. Jagendorf, Ionic and pH transitions triggering chloroplast post-illumination luminescence, Arch. Biochem. Biophys. 129 (1969) 711–719.
[24] J. Barber, G.P. Kraan, Salt-induced light emission from chloroplasts, Biochim. Biophys. Acta 197 (1970) 49–59.
[25] A.R. Crofts, C.A. Wraight, D.E. Fleischmann, Energy conservation in the photochemical reactions of photosynthesis and its relation to delayed fluorescence, FEBS Lett. 15 (1971) 89–100.
[26] A. Cuni, L. Xiong, R. Sayre, F. Rappaport, J. Lavergne, Modification of the pheophytin midpoint potential in photosystem II: modulation of the quantum yield of charge separation and of charge recombination pathways, Phys. Chem. Chem. Phys. 6 (2004) 4825–4831.
[27] H. Schliephake, W. Junge, H.T. Witt, Z. Naturforsch. 23b (1968) 1571–1578.
[28] A.A. Bulychev, W.J. Vredenberg, Effect of ionophores A23187 and nigericin on the light-induced redistribution of Mg2+, K+ and H+ across the thylakoid membrane, Biochim. Biophys. Acta 449 (1976) 48–58.
[29] J. Teissie, Interaction of cytochrome *c* with phospholipid monolayers. Orientation and penetration of protein as functions of the packing density of film, nature of the phospholipids, and ionic content of the aqueous phase, Biochemistry 20 (1981) 1554–1560.
[30] J. Teissie, M.P. Rols, An experimental evaluation of the critical potential difference inducing cell membrane electropermeabilization, Biophys. J. 65 (1993) 409–413.
[31] U. Schreiber, Detection of rapid induction kinetics with a new type of high-frequency modulated chlorophyll fluorimeter, Photosynth. Res. 9 (1986) 261–272.
[32] R.J. Strasser, Govindjee. (1992) (M. Murata, ed.), Vol. 2, pp. 29–32, Kluwer, Dordrecht.
[33] R.J. Strasser, Govindjee. (1991) (J.H. Argyroudi-Akoyunoglou, ed.), pp. 423–426, Plenum Press, New York.
[34] P. Joliot, A. Joliot, Cyclic electron flow in C3 plants, Biochim. Biophys. Acta 1757 (2006) 362–368.
[35] P. Turina, D. Samoray, P. Graber, H+/ATP ratio of proton transport-coupled ATP synthesis and hydrolysis catalysed by CF0F1-liposomes, EMBO J. 22 (2003) 418–426.
[36] J. Rosing, E.C. Slater, The value of G degrees for the hydrolysis of ATP, Biochim. Biophys. Acta 267 (1972) 275–290.